Second Virial Coefficient of Oligo- and Polystyrenes near the Θ Temperature. More on the Coil-to-Globule Transition

Hiromi Yamakawa,* Fumiaki Abe, and Yoshiyuki Einaga

Department of Polymer Chemistry, Kyoto University, Kyoto 606-01, Japan

Received May 10, 1994; Revised Manuscript Received July 11, 1994®

ABSTRACT: The second virial coefficient A_2 was determined for atactic oligo- and polystyrenes in cyclohexane below, at, and above Θ in the range of weight-average molecular weight M_w from 3.70×10^2 to 4.00×10^4. It is found that A_2 increases significantly with decreasing M_w at any temperature T for $M_w < 5 \times 10^3$, while this dependence almost disappears for larger M_w below Θ, in agreement with the literature results. It is then shown that such molecular-weight dependence of A_2 may be explained quantitatively by the Yamakawa theory that takes account of the effect of chain ends. An analysis gives values of the effective excess binary-cluster integrals β_1 and β_2 associated with the chain end beads and also the binary-cluster integral β between intermediate identical beads as functions of T, all of them except for β above Θ being quadratic in $\tau = 1 - \Theta/T$. With these values of β, the conventional and scaled excluded-volume parameters z and $\tilde{z}$ below Θ are recalculated. The results for the part $A_2^{(HW)}$ of A_2 without the effect of chain ends give a single composite curve below Θ when $A_2^{(HW)}M_w^{1/2}$ is plotted against z, being consistent with the two-parameter theory prediction. The deviation of the $A_2M_w^{1/2}$ vs z plot or the A_2 vs $|\tau|$ plot from this prediction previously reported arises not only from the effect of chain ends but also from the previous assumption of the proportionality of β and hence z to τ. The present and literature findings of the M_w independence of A_2 itself (except for small M_w) below Θ are due to a cancellation of the M_w dependence of $A_2^{(HW)}$ by that of the effect of chain ends. The composite curve above and also that of the gyration-radius expansion factor α_S vs $\tilde{z}$ below Θ are found to be close to the respective first-order perturbation theory values. With these results, a supplementary discussion of the coil-to-globule transition is also given.

Introduction

Recently, Yamakawa[1] has investigated theoretically the second virial coefficient A_2 and radius expansion factor α_S for flexible polymers below the Θ temperature within the new framework of a theory[2] based on the helical wormlike (HW) chain.[3,4] The main problem of A_2 below Θ is to explain its molecular-weight M independence as observed for atactic polystyrene (a-PS),[5,6] which is inconsistent with the two-parameter theory prediction.[7] According to the new theory,[2] the chain stiffness has a significant effect on A_2 or the interpenetration function Ψ appearing in it even for large M and, on the other hand, the effect of chain ends also becomes appreciable for relatively small M. Indeed, it has already been shown[8-10] that the former effect explains well, although not quantitatively, the experimental result that Ψ is not a universal function of α_S, while the latter explains satisfactorily the strong M dependence of A_2 observed for small M at Θ (at which A_2 vanishes for large M) and also in good solvents. These findings are also inconsistent with the two-parameter theory prediction. As for A_2 below Θ, from an analysis of the literature data[5,11] for a-PS by the use of the new theory, it has been suggested that the M independence of A_2 may be explained by taking account of the effect of chain ends but not of chain stiffness.[1] However, an accurate determination of the effect of chain ends on A_2 below Θ has been difficult because of the lack of data for A_2 for small M.

Thus, in the present work, we determine A_2 for a-PS in cyclohexane below and also above Θ in the range of small M, including the oligomers. (The problem of A_2 at Θ has already been resolved, as mentioned above.[9]) We evaluate first the contribution $A_2^{(E)}$ of the effect of chain ends to A_2 below and above Θ and then that part $A_2^{(HW)}$ of A_2 without this effect which vanishes at Θ. The excluded-volume strength B or the binary-cluster integral β is then determined as a function of temperature from A_2 in the oligomer region in which $A_2^{(HW)}$ is independent of M. This enables us to calculate the conventional excluded-volume parameter z and the scaled excluded-volume parameter $\tilde{z}$ without any assumption. Thus we obtain values of $A_2^{(HW)}M^{1/2}$ and α_S as functions of z or $\tilde{z}$ to compare them with the theory. With these results, a supplementary discussion of the coil-to-globule transition is also given.

Experimental Section

Materials. Most of the a-PS samples used in this work are the same as those used in the previous studies of the mean-square optical anisotropy $\langle\Gamma^2\rangle$,[12] the intrinsic viscosities $[\eta]_\Theta$[13] and $[\eta]$,[14,15] the mean-square radii of gyration $\langle S^2\rangle_0$[16] and $\langle S^2\rangle$,[17] the scattering function $P_s(k)$,[18] the translational diffusion coefficient D,[19] and A_2 (or Ψ),[8,9] i.e., the fractions separated by preparative gel permeation chromatography (GPC) or fractional precipitation from the standard samples supplied by Tosoh Co., Ltd. In this work, however, some additional samples were prepared similarly by separation from the Tosoh standard samples. All the samples have a fixed stereochemical composition (the fraction of racemic diads $f_r = 0.59$) independent of molecular weight, possessing an n-butyl group at one end of the chain (the initiating end) and a hydrogen atom at the other (the terminating end).

The values of the weight-average molecular weight M_w, the weight-average degree of polymerization x_w, and the ratio of M_w to the number-average molecular weight M_n are listed in Table 1. Samples OS8a, A2500a-2, F1a-2, and F2-2 are the additional ones, and their M_ws were determined from light scattering (LS) measurements in cyclohexane at 34.5 °C (Θ). As seen from the values of M_w/M_n, all the samples are sufficiently narrow in molecular weight distribution, and, in particular, samples OS3, OS4, and OS5 are completely monodisperse.

The solvent cyclohexane was purified according to a standard procedure prior to use.

Light Scattering. LS measurements were carried out to determine A_2 (and also M_w) for all the a-PS samples in cyclohexane at various temperatures ranging from 15.0 to 50.0 °C. A Fica 50 light-scattering photometer was used for all the measurements with vertically polarized incident light of wavelength 436 nm. For a calibration of the apparatus, the intensity of light scattered from pure benzene was measured at 25.0 °C at a scattering angle

® Abstract published in *Advance ACS Abstracts*, September 1, 1994.

0024-9297/94/2227-5704$04.50/0

Table 1. Values of M_w, x_w, and M_w/M_n for Atactic Oligo- and Polystyrenes

sample	M_w	x_w	M_w/M_n
OS3[a]	3.70×10^2	3	1.00
OS4	4.74×10^2	4	1.00
OS5	5.78×10^2	5	1.00
OS6	6.80×10^2	5.98	1.00
OS8a	9.20×10^2	8.29	1.01
A1000-a[b]	1.23×10^3	11.3	1.03
A2500a-2	2.83×10^3	26.7	1.03
A5000-3[c]	5.38×10^3	51.2	1.03
Fla-2	9.98×10^3	95.4	1.03
F2-2	2.02×10^4	194	1.02
F4[b]	4.00×10^4	384	1.02

[a] M_ws of OS3 through OS6 had been determined from GPC.[12,13] [b] M_ws of A1000-a and F4 had been determined from LS in cyclohexane at 34.5 °C.[15,16] [c] M_w of A5000-3 had been determined from LS in methyl ethyl ketone at 25.0 °C.[12]

of 90°, where the Rayleigh ratio R_{Uu} (90°) of pure benzene was taken as 46.5×10^{-6} cm^{-1}. The depolarization ratio ρ_u of pure benzene at 25.0 °C was determined to be 0.41 ± 0.01 by the method of Rubingh and Yu.[20]

The conventional method was used for solutions of the samples with $M_w > 10^3$, while the new procedure previously[21] presented was applied to those of the oligomer samples with $M_w < 10^3$ as before[9,10] since then the concentration dependences of the density scattering R_d and the optical constant K have significant effects on the determination of A_2 (and also of M_w). To determine A_2 by the latter procedure, we measured the reduced total intensity R_{Uv}* of the unpolarized scattered light for vertically polarized incident light, the depolarization ratio ρ_u, the ratio $\kappa_T/\kappa_{T,0}$ of the isothermal compressibility of a given solution to that of the solvent, and the refractive index increment $(\partial\tilde{n}/\partial c)_{T,p}$ at constant (absolute) temperature T and pressure p for the oligomer solutions and also the first two quantities for the solvent. The values of the refractive index $\tilde{n}$ at finite concentrations c, which were required to calculate K, were calculated with the values of $(\partial\tilde{n}/\partial c)_{T,p}$ for each oligomer sample, as described in the Results section. Measurements of R_{Uv}* were carried out at scattering angles θ ranging from 45 to 135°, and the mean of the values obtained at different θ was adopted as its value, since it must be independent of θ for oligomers. The values of ρ_u were obtained by the same method as employed in the calibration of the apparatus.

All the LS data obtained were analyzed by using the Berry square-root plot[22] and also the Bawn plot.[23,24]

The most concentrated solutions of each sample were prepared by continuous stirring at ca. 50 °C for 1–4 days. They were optically purified by filtration through a Teflon membrane of pore size 0.45 or 0.10 μm. The solutions of lower concentrations were obtained by successive dilution. The polymer mass concentrations c were calculated from the weight fractions with the densities of the solutions. The densities of the solvents and solutions were measured with a pycnometer of the Lipkin–Davison type.

Isothermal Compressibility. Isothermal compressibility measurements were carried out to determine $\kappa_T/\kappa_{T,0}$ for oligomer sample OS4 in cyclohexane at 15.0 and 50.0 °C. The apparatus and the method of measurements are the same as those described in the previous paper.[9] This ratio was determined as a function of c and p. The latter was varied from 1 to ca. 50 atm. In this range of p, it was independent of p within experimental error, so that we adopted the mean of the values obtained at various pressures as its value at 1 atm.

Refractive Index Increment. The refractive index increment $(\partial\tilde{n}/\partial c)_{T,p}$ was determined as a function of c and T for each oligomer sample for $M_w < 3 \times 10^3$ at temperatures ranging from 15.0 to 50.0 °C by the use of a Shimadzu differential refractometer.

Results

Light Scattering from Oligostyrene Solutions. In this subsection we give the results for $\kappa_T/\kappa_{T,0}$ and $(\partial\tilde{n}/\partial c)_{T,p}$ and the LS data for the oligomer samples with $M_w \leq 5.38 \times 10^3$. Figure 1 shows plots of $\kappa_T/\kappa_{T,0}$ against c for

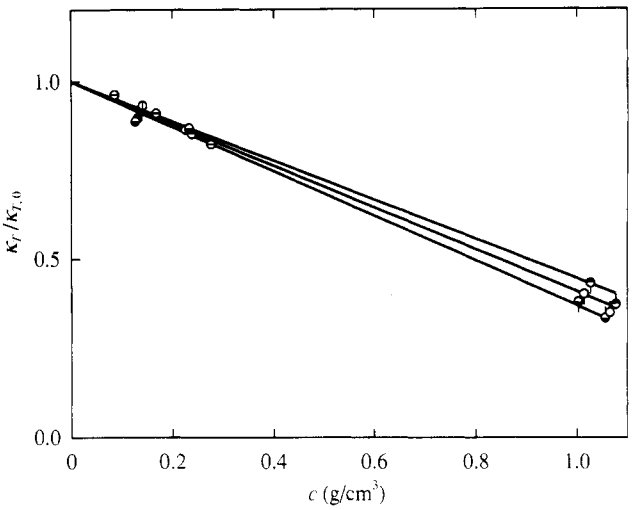

Figure 1. Plots of $\kappa_T/\kappa_{T,0}$ against c for a-PS in cyclohexane: (●) OS4 at 15.0 °C; (◒) OS4 at 50.0 °C; (⊖) OS2 (M = 266) at 34.5 °C;[9] (⊕) OS3 at 34.5 °C;[9] (pip down) x_w = 2–5 in the bulk at 15.0 (◒), 34.5 (○), and 50.0 °C (◒);[25] (pip up) $M_n = 5.1 \times 10^4$ and 8.2×10^4 in the bulk at 15.0 (◓), 34.5 (◯), and 50.0 °C (◓)[26] (see text).

Table 2. Values of k_1 in Equation 2 for Atactic Oligostyrene in Cyclohexane

sample	k_1, cm^3/g	sample	k_1, cm^3/g
OS3	0.146	OS8a	0.171_5
OS4	0.154	A1000-a	0.176_5
OS5	0.157_5	A2500a-2	0.179
OS6	0.163_5		

sample OS4 in cyclohexane at 15.0 (top-half-filled circles) and 50.0 °C (bottom-half-filled circles) along with the literature data obtained by Allen et al.[25] (circles with pip down) for a mixture of styrene oligomers including the dimer through the pentamer in the bulk and by Höcker et al.[26] (circles with pip up) for high-molecular-weight samples with $M_n = 5.1 \times 10^4$ and 8.2×10^4 in the bulk. For these literature data, the values of $\kappa_T/\kappa_{T,0}$ have been calculated by the use of the values of $\kappa_{T,0}$ given by Holder and Whalley[27] for pure cyclohexane at the respective temperatures and the densities have been taken as the values of c. The figure also includes the results obtained previously[9] for OS2 (M = 266) (circles with horizontal bar) and OS3 (circles with vertical bar) in cyclohexane at 34.5 °C and the literature data by the above authors[25,26] (unfilled circles) for their respective samples at 34.5 °C.

As seen from Figure 1, the plot of $\kappa_T/\kappa_{T,0}$ against c at each temperature follows a single straight line irrespective of the difference in molecular weight and may then be represented by the equation

$$\kappa_T/\kappa_{T,0} = 1 + kc \tag{1}$$

where the values of k determined from the straight lines indicated are −0.554, −0.591, and −0.630 cm^3/g at 15.0, 34.5, and 50.0 °C, respectively. It is also seen that for $c < 0.3$ g/cm^3, where LS measurements for the oligomer samples were carried out, the variation of $\kappa_T/\kappa_{T,0}$ with temperature is very small and almost within experimental uncertainty. Thus we have evaluated $\kappa_T/\kappa_{T,0}$ at temperatures ranging from 15.0 to 50.0 °C except at 34.5 °C by interpolation using eq 1 with the values of k above.

The results for $(\partial\tilde{n}/\partial c)_{T,p}$ at 436 nm for each oligomer sample in cyclohexane are independent of c for $c < 0.15$ g/cm^3 and may be expressed as a function of T by the equation

$$(\partial\tilde{n}/\partial c)_{T,p} = k_1 + k_2(T - \Theta) \tag{2}$$

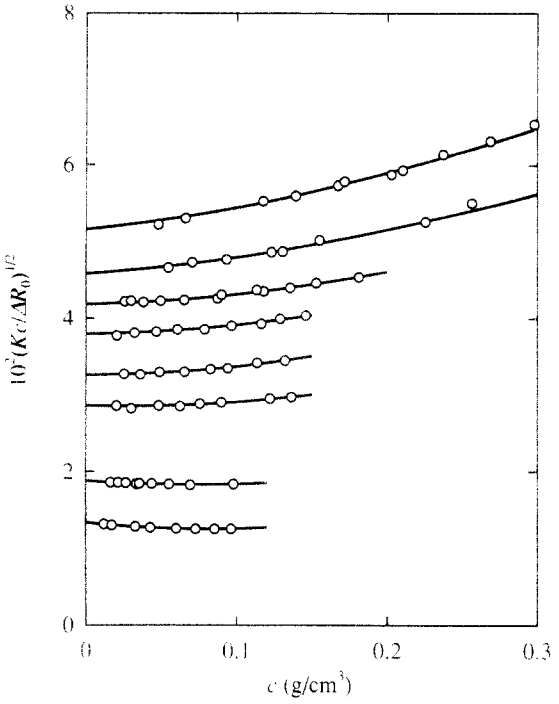

Figure 2. Plots of $(Kc/\Delta R_0)^{1/2}$ against c for a-PS in cyclohexane at 15.0 °C. The samples are OS3, OS4, OS5, OS6, OS8a, A1000-a, A2500a-2, and A5000-3 from top to bottom.

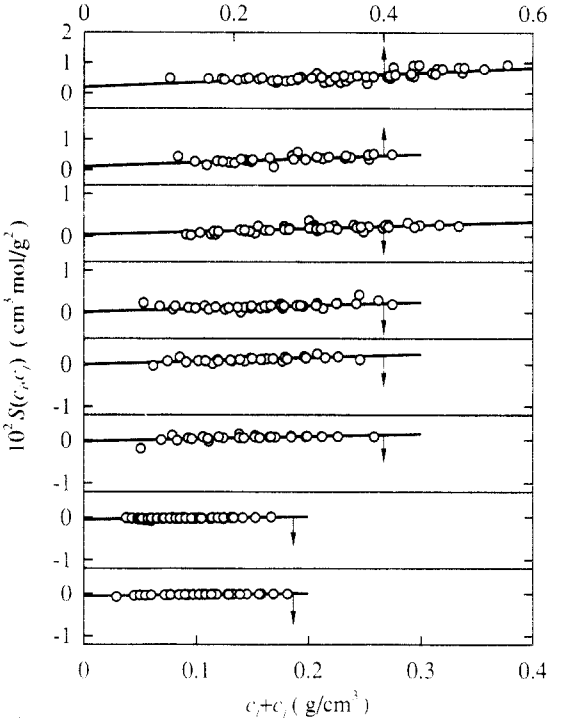

Figure 3. Bawn plots for a-PS in cyclohexane at 15.0 °C. The samples are OS3, OS4, OS5, OS6, OS8a, A1000-a, A2500a-2, and A5000-3 from top to bottom.

where k_2 is independent of M_w and equal to $(3.7 \pm 0.5) \times 10^{-4}$ cm³/g K but k_1 depends on M_w.[28] The values of k_1 determined for the oligomer samples are listed in Table 2. We note that the value of k_1 is 0.181 cm³/g independently of M_w for $M_w \gtrsim 5 \times 10^3$. The values of $\tilde{n}$ at finite c may be obtained from eq 2 by integration over c with the values of $\tilde{n}_0$ for pure cyclohexane at the respective temperatures corresponding to the LS measurements.

Figure 2 shows as examples Berry square-root plots of the excess Rayleigh ratio ΔR_0 against c for the oligomer samples with $M_w \leq 5.38 \times 10^3$ in cyclohexane at 15.0 °C. The data points for each sample follow a curve concave upward, as shown by the solid curve (which represents the values calculated as described below). The results imply that besides the second virial coefficient A_2', the third virial coefficient A_3' at least makes a significant contribution to $Kc/\Delta R_0$ as c is increased. (Here, the prime attached to A_2 and A_3 indicates that they are the *light-scattering* virial coefficients.) It is then difficult to determine A_2' from the plots with sufficient accuracy.

Therefore, we have made Bawn plots of these data as indicated in Figure 3, where $S(c_i,c_j)$ is defined by eq 6 of ref 10. As seen from this figure, the data points for each sample follow a straight line, indicating that terms higher than A_3' may be neglected in the range of c studied. From the straight lines indicated, we have determined A_2' and A_3' for each sample in cyclohexane at 15.0 °C. Then we have determined M_w of each sample so that the curve of $(Kc/\Delta R_0)^{1/2}$ calculated with these values of M_w, A_2', and A_3' may give a best fit to the data points in Figure 2. The solid curves in Figure 2 represent the values thus calculated. The good fit of each curve to the corresponding data points indicates that M_w, A_2', and A_3' have been determined with sufficient accuracy.

Although the results are not shown here, the data at the other temperatures and for the samples with higher molecular weights have been analyzed by the same method, and the values of M_w, A_2', and A_3' have been determined with an accuracy comparable to or better than the cases of Figures 2 and 3. It has proved that the values of A_2' thus obtained may be equated to those of the (osmotic) second virial coefficient A_2 as in the case of the previous results at Θ.[9]

Table 3. Results for A_2 of Atactic Oligo- and Polystyrenes in Cyclohexane

	$10^4 A_2$, cm³ mol/g²							
sample	15.0 °C	20.0 °C	25.0 °C	30.0 °C	34.5 °C (Θ)	40.0 °C	45.0 °C	50.0 °C
OS3	10	13	15	18	21	22	24	26
OS4	5.0	7.0	9.0	11	13	14	16	17
OS5	2.0	4.7	6.2	8.5	11.0	12.0	12.8	13.5
OS6	1.2	3.0	5.0	7.0	8.3	9.5	10.7	11.8
OS8a	0.0	1.2	3.0	4.2	6.0	7.0	8.0	9.0
A1000-a	−1.30	0.20	1.50	2.90	4.10[a]	4.70	5.40	6.30
A2500-a					1.33[a]			
A2500a-2	−2.3	−1.46	−0.64	0.10	0.60	1.23	1.74	2.14
A5000-3	−2.75	−1.83	−1.03	−0.40	0.25	0.75	1.20	1.70
F1a-2	−2.70	−2.00	−1.20	−0.45	0.15	0.60	0.88	1.25
F1-2					0.28[a]			
F2					0.10[a]			
F2-2	−2.57	−1.80	−1.10	−0.39	0.07	0.47	0.83	1.17
F4	−2.58	−1.65	−0.91	−0.39	0.03	0.40	0.77	1.10

[a] Reproduced from ref 9.

Second Virial Coefficient. The values of A_2 determined from LS measurements for all the samples in cyclohexane at temperatures ranging from 15.0 to 50.0 °C are summarized in Table 3, where some of the results previously obtained at 34.5 °C (Θ) are also included. They are plotted against $1/T$ in Figure 4 (except for A2500-a, F1-2, and F2). The solid curves connect the data points smoothly. It is seen that at $T < \Theta$ A_2 does not vary appreciably with M_w for $M_w > 5 \times 10^3$. This result is consistent with the above-mentioned findings by Tong et al.[5] and by Perzynski et al.[6] However, in a wider range of M_w including the oligomers, A_2 depends significantly on M_w even at $T < \Theta$, in contradiction to their conclusion. It is clearly seen that for $M_w \leq 2.83 \times 10^3$ A_2 increases progressively with decreasing M_w at any temperature examined. Corresponding to this, the temperature at which A_2 vanishes decreases with decreasing M_w.

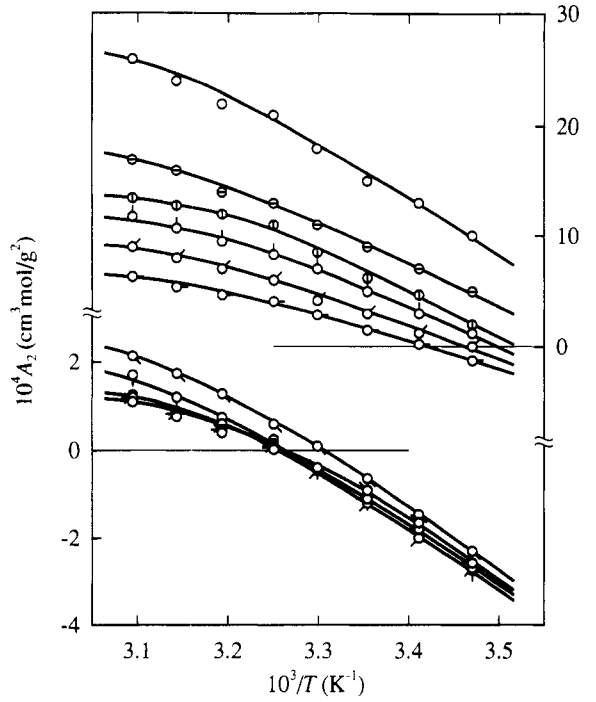

Figure 4. Plots of A_2 against $1/T$ for a-PS in cyclohexane: (○) OS3; (⊖) OS4; (⏀) OS5; (♀) OS6; successive 45° clockwise rotations of pips indicate OS8a, A1000-a, A2500a-2, A5000-3, F1a-2, F2-2, and F4, respectively. The solid curves connect the data points smoothly.

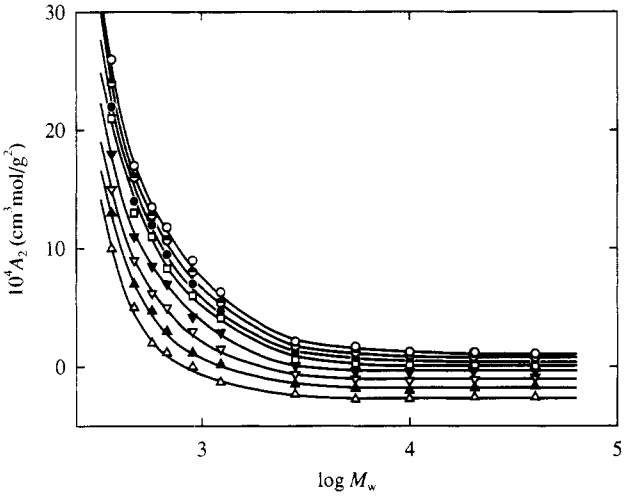

Figure 5. Plots of A_2 against log M_w for a-PS in cyclohexane: (○) at 50.0 °C; (◓) at 45.0 °C; (●) at 40.0 °C; (□) at 34.5 °C (Θ); (▼) at 30.0 °C; (▽) at 25.0 °C; (▲) at 20.0 °C; (△) at 15.0 °C. The solid curves connect the data points smoothly.

In Figure 5, the values of A_2 at all temperatures studied are plotted against log M_w for the same samples as in Figure 4. The solid curves connect the data points smoothly. For $M_w \lesssim 2 \times 10^3$, A_2 increases steeply with decreasing M_w at any temperature, while it is nearly constant for $M_w > 5 \times 10^3$ at $T < \Theta$, as stated above. It has already been shown in the previous paper[9] that the dependence of A_2 on M_w at Θ may be quantitatively explained by the Yamakawa theory[2] that takes account of the effect of chain ends. The sharp increase in A_2 for small M_w at the other temperatures may also be regarded as arising from the same effect.

Discussion

Effects of Chain Ends on A_2. We analyze the data for A_2 in Table 3 by the use of the Yamakawa theory[2] that considers the effect of chain ends on the basis of the HW touched-bead model. It is such that $n+1$ beads are arrayed with spacing a between them along the contour of total length $L = na$, where the $n-1$ intermediate beads are identical and the two end ones are different from the intermediate ones and also from each other in species. Identical excluded-volume interactions are expressed in terms of the conventional binary-cluster integral β, while two kinds of effective excess binary-cluster integrals, β_1 and β_2, are necessary to express interactions between unlike beads, β_1 being associated with one end bead and β_2 with two end beads. The HW model itself[3,4] is defined in terms of the three basic model parameters: the constant differential-geometrical curvature κ_0 and torsion τ_0 of its characteristic helix and the static stiffness parameter λ^{-1}.

According to the theory,[2] A_2 in general may be written in the form

$$A_2 = A_2^{(HW)} + A_2^{(E)} \tag{3}$$

where $A_2^{(HW)}$ is that part of A_2 without the effect of chain ends which vanishes at Θ and $A_2^{(E)}$ represents the contribution of this effect to A_2. The first term $A_2^{(HW)}$ may be written as

$$A_2^{(HW)} = (N_A c_\infty^{3/2} L^2 B/2M^2)h \tag{4}$$

where N_A is Avogadro's number and c_∞ and B are given by

$$c_\infty = \frac{4 + (\lambda^{-1}\tau_0)^2}{4 + (\lambda^{-1}\kappa_0)^2 + (\lambda^{-1}\tau_0)^2} \tag{5}$$

and

$$B = \beta/a^2 c_\infty^{3/2} \tag{6}$$

For the conventional excluded-volume parameter $z > 0$ with z being now defined by

$$z = (3/2\pi)^{3/2}(\lambda B)(\lambda L)^{1/2} \tag{7}$$

the h function is given by

$$h(\hat{z}) = (1 + 7.74\hat{z} + 52.3\hat{z}^{27/10})^{-10/27} \tag{8}$$

with

$$\hat{z} = \tilde{z}/\alpha_S^3 \tag{9}$$

In eq 9, $\tilde{z}$ is the intermolecular scaled excluded-volume parameter defined by[1]

$$\tilde{z} = [Q(\lambda L)/2.865]z \tag{10}$$

where Q is a function only of λL for ordinary flexible polymers and given by eq 19 of ref 2 for $\lambda L \gtrsim 1$. We may assume that α_S^2 ($=\langle S^2\rangle/\langle S^2\rangle_0$) is a function only of $\tilde{z}$ and adopt the Domb–Barrett equation[29] for it for $z > 0$ with the intramolecular scaled excluded-volume parameter $\tilde{z}$ in place of z,

$$\alpha_S^2 = [1 + 10\tilde{z} + (70\pi/9 + 10/3)\tilde{z}^2 + 8\pi^{3/2}\tilde{z}^3]^{2/15} \times [0.933 + 0.067\exp(-0.85\tilde{z} - 1.39\tilde{z}^2)] \tag{11}$$

where $\tilde{z}$ is defined by

$$\tilde{z} = (3/4)K(\lambda L)z \tag{12}$$

with K being a function only of λL and given by eq 9 of ref 2.

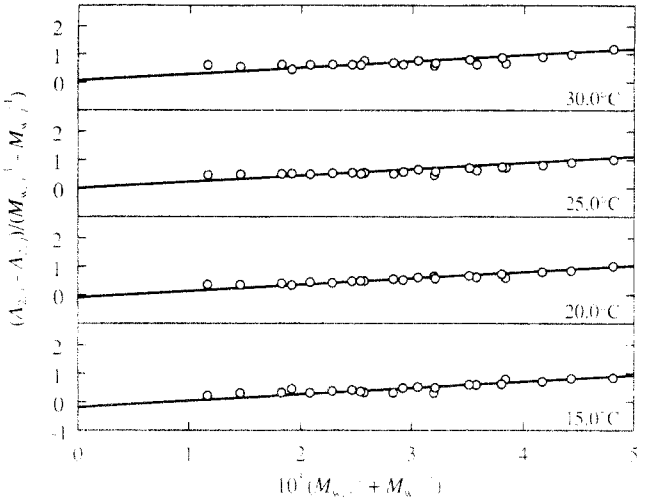

Figure 6. Plots of $(A_{2,i} - A_{2,j})/(M_{w,i}^{-1} - M_{w,j}^{-1})$ against $M_{w,i}^{-1} + M_{w,j}^{-1}$ for a-PS in cyclohexane at $T < \Theta$ (see text).

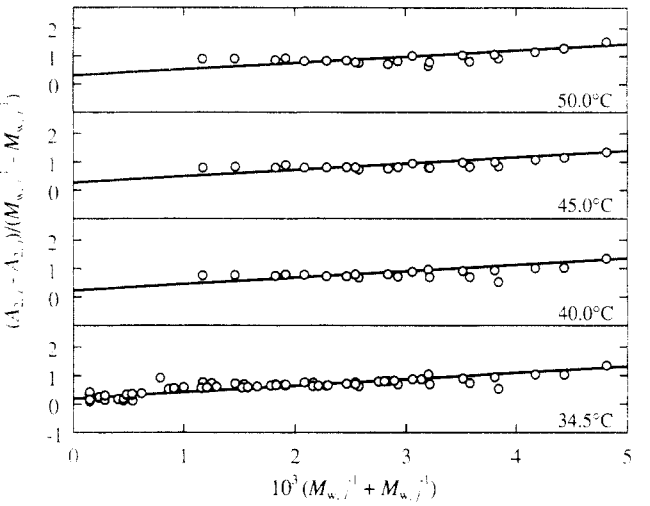

Figure 7. Plots of $(A_{2,i} - A_{2,j})/(M_{w,i}^{-1} - M_{w,j}^{-1})$ against $M_{w,i}^{-1} + M_{w,j}^{-1}$ for a-PS in cyclohexane at $T \geq \Theta$ (see text).

For $z < 0$, for convenience, we adopt the equation

$$h = 1 - 2.865\tilde{z} + 8.851\tilde{z}^2 + 5.077\tilde{z}\tilde{z} - \ldots \quad (13)$$

derived from the perturbation theory, since the function h given by eq 8 has a singularity at $z = 0$.[1]

Thus, note that h is a function of $\tilde{z}$ and $\tilde{z}$ for $z \gtrless 0$ and that we may put $h = 1$ approximately for $\lambda L \lesssim 1$. Recall that L is related to M by the equation

$$L = M/M_L \quad (14)$$

with M_L the shift factor as defined as the molecular weight per unit contour length.

The second term $A_2^{(E)}$ in eq 3 may be written in the form

$$A_2^{(E)} = a_1 M^{-1} + a_2 M^{-2} \quad (15)$$

where

$$a_1 = 2N_A\beta_1/M_0$$

$$a_2 = 2N_A\Delta\beta_2 \quad (16)$$

with M_0 the molecular weight of the bead and with

$$\Delta\beta_2 = \beta_2 - 2\beta_1 \quad (17)$$

The parameters β_1 and β_2 are explicitly defined in eqs 22 of ref 2.

Now, in the oligomer region where the relation $h = 1$ holds, $A_2^{(HW)}$ is independent of M, so that we have from eqs 3 and 15

$$(A_{2,i} - A_{2,j})/(M_i^{-1} - M_j^{-1}) = a_1 + a_2(M_i^{-1} + M_j^{-1}) \quad (18)$$

with $A_{2,i}$ and $A_{2,j}$ the second virial coefficients for the samples with different molecular weights M_i and M_j, respectively. Equation 18 indicates that a_1 and a_2 may be determined from the intercept and slope of the plot of $(A_{2,i} - A_{2,j})/(M_{w,i}^{-1} - M_{w,j}^{-1})$ vs $M_{w,i}^{-1} + M_{w,j}^{-1}$, respectively. Figures 6 and 7 show such plots for the present data at $T < \Theta$ and at $T \geq \Theta$, respectively, for the low-molecular-weight samples with $M_w \leq 2.83 \times 10^3$, for which h may be equated to unity. We note that the plots at 34.5 °C (Θ) include the present and previous[9] data for all the samples given in Table 3, since $A_2^{(HW)} = 0$ at $T = \Theta$ and then eq 18 holds irrespective of the values of M_w. As expected,

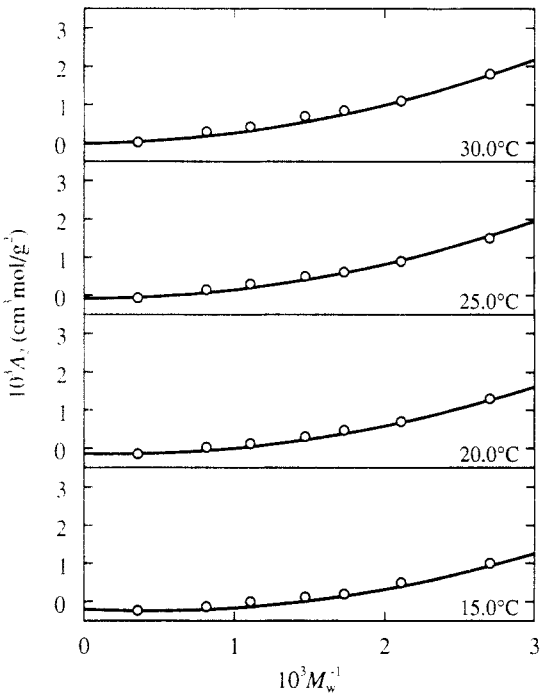

Figure 8. Plots of A_2 against M_w^{-1} for a-PS in cyclohexane at $T < \Theta$ (see text).

the data points at each temperature can be fitted by a straight line. The results confirm that the upswing of A_2 for small M_w shown in Figure 5 arises from the effect of chain ends. From the straight lines indicated, we have determined a_1 and a_2 at the respective temperatures. It has then been found that a_2 is a constant independent of T.

Figures 8 and 9 show plots of A_2 against M_w^{-1} with the data corresponding to those in Figures 6 and 7, respectively. From the plots, we have determined $A_2^{(HW)}$ with $h = 1$ at each temperature so that the curve of A_2 as a function of M_w^{-1} calculated from eqs 3 and 15 with these values of $A_2^{(HW)}$ (with $h = 1$), a_1, and a_2 may give a best fit to the data points. The solid curves in Figures 8 and 9 represent the values thus calculated. The good agreement between the calculated and observed values again indicates that the dependence of A_2 on M_w for small M_w arises from the effect of chain ends. Note that the intercept of each solid curve is equal to $A_2^{(HW)}$ with $h = 1$, i.e., the prefactor $(N_A c_\infty^{3/2} L^2 B/2M^2)$, from which we have determined B at the corresponding temperature.

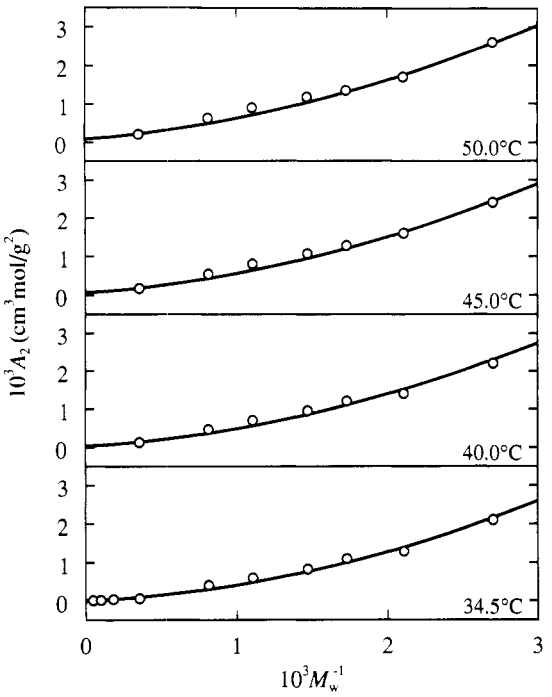

Figure 9. Plots of A_2 against M_w^{-1} for a-PS in cyclohexane at $T \geq \Theta$ (see text).

Temperature Dependence of Binary-Cluster Integrals. With the values of B, a_1, and a_2 obtained in the last subsection, we have calculated β, β_1, and β_2 at the respective temperatures from eqs 6 and 16 with eq 17 by taking the repeat unit of the chain as a single bead (M_0 = 104). For the calculation of β, we have used the values of the HW model parameters determined previously[12,17] from $\langle\Gamma^2\rangle$ and $\langle S^2\rangle_0$, i.e., $\lambda^{-1}\kappa_0 = 3.0$, $\lambda^{-1}\tau_0 = 6.0$, $\lambda^{-1} = 20.6$ Å, and $M_L = 35.8$ Å^{-1}.

The values of β obtained at various temperatures above and below Θ are represented by the unfilled circles in Figure 10, where τ is defined by

$$\tau = 1 - \Theta/T \tag{19}$$

It also includes the values determined by Miyaki and Fujita[30] (filled circles) from α_S. (We note that their values of β plotted in this figure are somewhat lower than the original values because of the difference between our and their coil-limiting values of $\langle S^2\rangle_0/x_w$.[17]) For $\tau \geq 0$ ($T \geq \Theta$), the present values of β from A_2 are in good agreement with theirs from α_S and are found to be proportional to τ. However, it is important to see that for $\tau < 0$, the plot deviates significantly downward from a linear extension of the straight line fitted to the data points for $\tau \geq 0$ (dashed line), the deviation being larger for lower T. With these results, for later use, we have constructed an empirical equation for β (in Å^3) as a function of τ as follows:

$$\beta = 65\tau \qquad \text{for } \tau \geq 0$$

$$= 65\tau - 610\tau^2 \qquad \text{for } \tau < 0 \tag{20}$$

The solid curve in Figure 10 represents the values calculated from these equations.

In Figure 11, the values of β_1 (unfilled circles) and β_2 (filled circles) are plotted against τ. They are of reasonable order of magnitude as the effective excess binary-cluster integrals associated with the chain end beads compared to those for small molecules.[31] The data points for each of β_1 and β_2 follow a curve convex upward. With these results, for later use, we have also constructed empirical

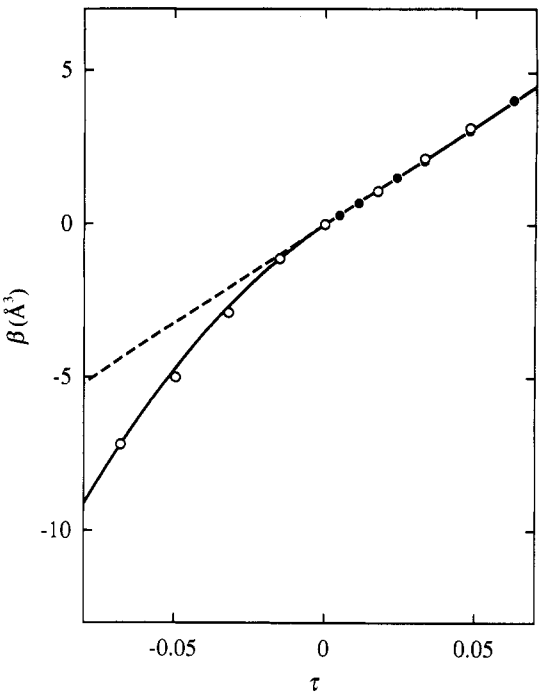

Figure 10. Plots of β against $\tau = 1 - \Theta/T$ for a-PS in cyclohexane: (○) present data from A_2; (●) results from Miyaki's data for α_S.[11] The solid curve represents the values calculated from eq 20. The dashed straight line is an extension of the solid line for $T > \Theta$ (see text).

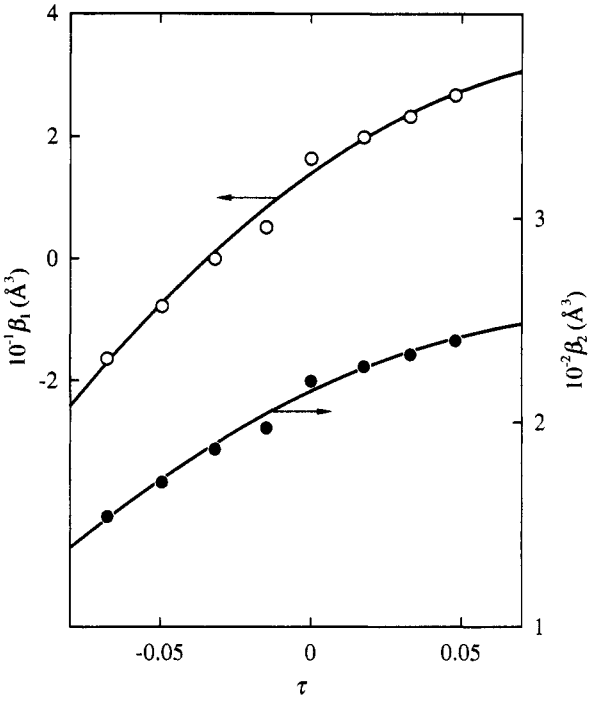

Figure 11. Plots of β_1 and β_2 against τ for a-PS in cyclohexane: (○) β_1; (●) β_2. The solid curves for β_1 and β_2 represent the values calculated from eqs 21 and 22, respectively.

equations for β_1 and β_2 (both in Å^3) as functions of τ as follows:

$$\beta_1 = 14 + 350\tau - 1600\tau^2 \tag{21}$$

$$\beta_2 = 215 + 700\tau - 3200\tau^2 \tag{22}$$

The sold curves for β_1 and β_2 in Figure 11 represent the values calculated from eqs 21 and 22, respectively.

Dependence of $A_2^{(HW)}M_w^{1/2}$ on z. In the previous paper,[1] values of $A_2M_w^{1/2}$ have been plotted against z for

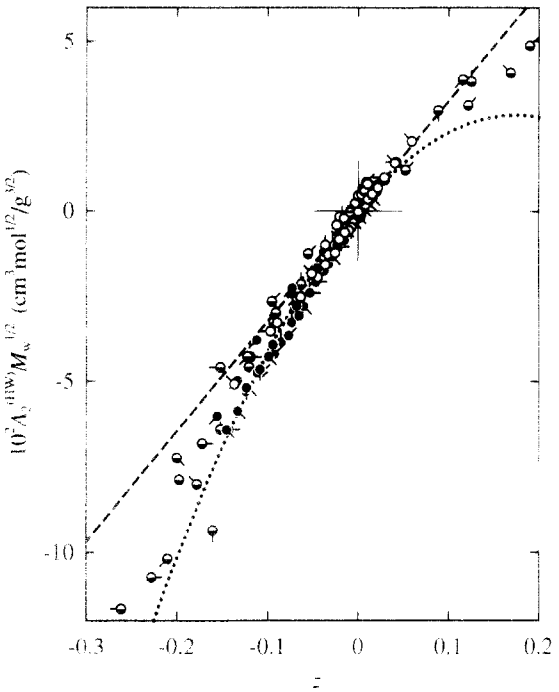

Figure 12. Plots of $A_2M_w^{1/2}$ against z for a-PS in cyclohexane: (○) present data (the symbols have the same meaning as those in Figure 4); (●) Tong et al.'s data for $10^4 \leq M_w \leq 4.91 \times 10^5$;[5] (◒) Miyaki's data for $1.34 \times 10^6 \leq M_w \leq 3.92 \times 10^7$.[11] Various directions of pips indicate different values of M_w. The dashed and dotted curves represent the values with $h = 1$ and the first-order two-parameter perturbation theory values, respectively (see text).

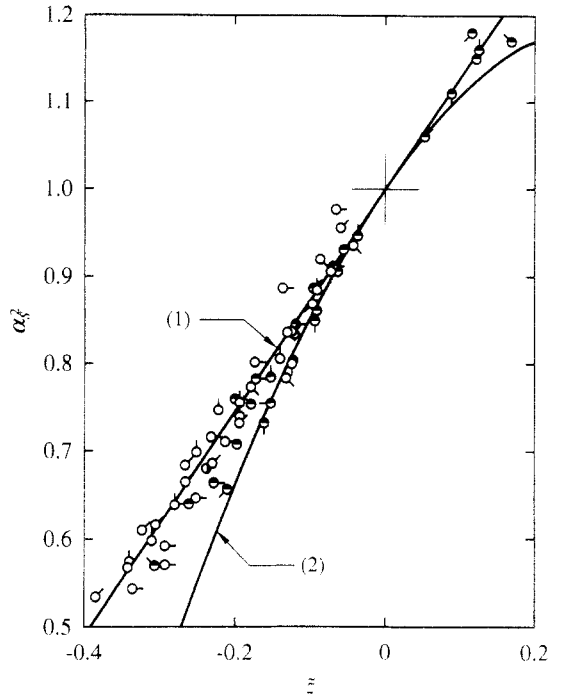

Figure 13. Plots of α_S^2 against $\tilde{z}$ for a-PS in cyclohexane: (◒) Miyaki's data for $1.34 \times 10^6 \leq M_w \leq 5.68 \times 10^7$;[11] (○) Park et al.'s data for $4.60 \times 10^6 \leq M_w \leq 4.09 \times 10^7$.[32,33] Various directions of pips indicate different values of M_w. The solid curves (1) and (2) represent the first- and second-order perturbation theory values, respectively.

a-PS in cyclohexane with the literature data by Tong et al.[5] for $10^4 \lesssim M_w \lesssim 5 \times 10^5$ and with those by Miyaki[11] for $M_w > 10^6$ (Figure 5 of ref 1). There, z has been calculated, assuming that β is proportional to τ for $\tau \gtrsim 0$, because of the lack of the data for β for $\tau < 0$. It has then been found that for $\tau < 0$ (below Θ), the data points for $M_w \gtrsim 5 \times 10^5$ form a single composite curve consistent with the two-parameter theory prediction, while those for $M_w < 5 \times 10^5$ deviate more and more downward from that curve as M_w is decreased and as T is lowered. From a theoretical consideration of the results, it has been suggested that the deviation may be explained by the effect of chain ends, as stated in the Introduction.

Now the results for β_1 and β_2 above allow us to determine the part $A_2^{(HW)}$ of A_2 without the effect of chain ends, and, moreover, those for β below Θ allow us to calculate z for $\tau < 0$ without the above assumption. Figure 12 shows plots of $A_2^{(HW)}M_w^{1/2}$ (with $A_2^{(HW)}$ in cm³ mol/g²) against the recalculated z with the present data (unfilled circles) along with the same literature data as cited in ref 1, i.e., those of Tong et al.[5] (filled circles) and Miyaki[11] (half-filled circles). (Note that we have obtained the values of $A_2^{(HW)}$ from A_2 by subtraction of $A_2^{(E)}$ calculated from eq 15 with eqs 16, 17, 21, and 22 and calculated z from eq 7 with eqs 6 and 20 and with the values of the HW model parameters given above.) The dashed straight line represents the theoretical values calculated from

$$A_2^{(HW)}M^{1/2} = 0.323zh \quad \text{(a-PS)} \tag{23}$$

with $h = 1$ (see eq 25 of ref 1), and the dotted curve represents the values calculated from eq 23 with the first-order two-parameter perturbation theory of h given by eq 13 with $\tilde{z} = \tilde{\tilde{z}} = z$ (i.e., $h = 1 - 2.865z$).

It is seen from Figure 12 that all the data points form nearly a single composite curve over the very wide range of M_w from 3.70×10^2 to 3.92×10^7, indicating that the effect of chain stiffness on $A_2^{(HW)}$ and hence A_2 is of little significance below Θ, in contrast to the behavior of A_2 above Θ, as pointed out previously[1] (compare with Figure 5 of ref 1). It is important to point out here that the deviation of the $A_2M_w^{1/2}$ vs z plot from the two-parameter theory prediction mentioned above arises not only from the effect of chain ends but also from the previous assumption of the proportionality of β and hence z to τ. The M_w independence of A_2 itself for a-PS for $M_w > 5 \times 10^3$ below Θ is due to a cancellation of the M_w dependence of $A_2^{(HW)}$ by that of $A_2^{(E)}$. It is also important to see from Figure 12 that the single composite curve fitted to the data points below Θ, although not explicitly shown, is located between the dashed and dotted curves and rather close to the latter, i.e., the first-order (two-parameter) perturbation theory values.

Coil-to-Globule Transition. In the previous paper,[1] we have constructed the plots of α_S^2 vs $\tilde{z}$ and of $\alpha_S^3|\tilde{z}|$ vs $|\tilde{z}|$ for a-PS in Θ solvents using the literature data of Miyaki[11] for $1.34 \times 10^6 \leq M_w \leq 5.68 \times 10^7$ and of Park et al.[32,33] for $4.60 \times 10^6 \leq M_w \leq 4.09 \times 10^7$ and concluded that the (quasi-) two-parameter scheme is still valid for α_S for flexible polymres below Θ (see Figures 3 and 4 of ref 1). There, $\tilde{z}$ has been calculated, assuming that β is proportional to τ as in the case of the $A_2M_w^{1/2}$ vs z plot. Thus, in this paper, we replot the same literature data for α_S for a-PS, although only in cyclohexane, by the use of the values of $\tilde{z}$ recalculated from eq 12 with β given by eq 20 (or the values of z obtained above). (Note that $\tilde{z}$ may be equated to z for these literature data for very large M_w.)

Figure 13 shows plots of α_S^2 against the recalculated $\tilde{z}$ with the data of Miyaki (half-filled circles) and Park et al. (unfilled circles). The solid curves (1) and (2) represent the first- and second-order perturbation theory values, respectively, calculated from

$$\alpha_S^2 = 1 + 1.276\tilde{z} - 2.082\tilde{z}^2 + \ldots \tag{24}$$

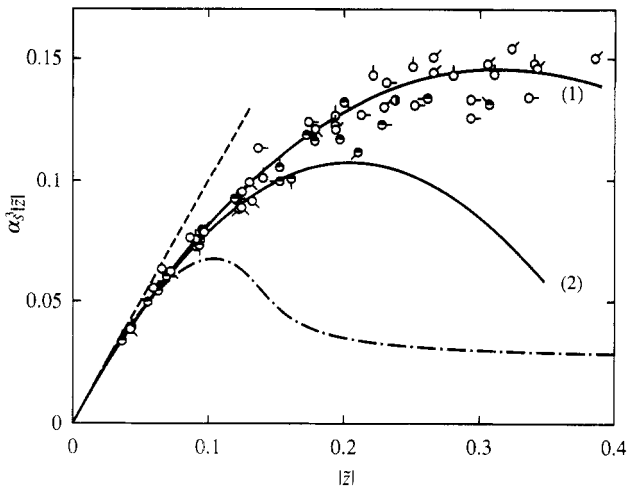

Figure 14. Plots of $\alpha_S^3|\tilde{z}|$ against $|\tilde{z}|$ for a-PS in cyclohexane. The symbols have the same meaning as those in Figure 13. The dashed straight line indicates the initial slope of unity. The solid curves (1) and (2) represent the first- and second-order perturbation theory values, respectively. The chain curve represents the values calculated from eq 25 with $z = \tilde{z}$ and $y = 0.07$.

(Recall that for $z < 0$ the α_S given by eq 11 has a singularity at $z = -0.1446$.[1]) All the data points again form a single composite curve within experimental error, confirming the validity of the (quasi-) two-parameter scheme for α_S. The composite curve, which is not shown explicitly, is located between the two curves and is close to the curve (1), i.e., the first-order perturbation theory values.

Figure 14 shows plots of $\alpha_S^3|\tilde{z}|$ against $|\tilde{z}|$ with the same data as in Figure 13 (except for those above Θ). The dashed straight line indicates the initial slope of unity, and the solid curves (1) and (2) correspond to those in Figure 13. The chain curve represents the values calculated from the mean-field theory equation

$$\alpha_S^5 - \alpha_S^3 - y\alpha_S^{-3} = 2.60z \qquad (25)$$

with $z = \tilde{z}$ and $y = 0.07$ as before,[1] where y is the parameter that arises from the ternary-cluster interaction. Necessarily, the data points are located near the solid curve (1), corresponding to the results in Figure 13, although they scatter somewhat.

With the reevaluation of the parameter $\tilde{z}$ (or z), the results shown in Figures 13 and 14 do not alter qualitatively the previous conclusion[1] concerning the coil-to-globule transition. That is, the globule state defined by the relation $\alpha_S^3|\tau|M^{1/2}$ = constant (the plateau region of the chain curve in Figure 14) cannot be realized experimentally for stable solutions of flexible polymers (except for biological macromolecules with specific intramolecular interactions). Now, very important and interesting is the fact that below Θ the first-order perturbation theory is approximately valid for α_S and also for A_2. Thus the future problem is to derive such closed expressions valid for them below Θ.

Concluding Remarks

It has been found that A_2 of a-PS below and above Θ depends significantly on M_w for $M_w < 5 \times 10^3$, while this dependence almost disappears below Θ for larger M_w, in agreement with the literature results.[5,6] The dependence of A_2 on M_w for small M_w may be explained quantitatively by the Yamakawa theory that takes account of the effect of chain ends. The analysis has allowed us to evaluate the contribution $A_2^{(E)}$ of this effect to A_2 at various temperatures, i.e., to determine the effective excess binary-cluster integrals β_1 and β_2 associated with the chain end beads as functions of temperature T. This has led to the evaluation of the binary-cluster integral β between intermediate identical beads as a function of T. With its values, the conventional and scaled excluded-volume parameters z and $\tilde{z}$ below Θ have been recalculated without any assumption. The part $A_2^{(HW)}$ of A_2 without the effect of chain ends obtained as $A_2^{(HW)} = A_2 - A_2^{(E)}$ is found to be consistent with the two-parameter theory prediction, giving a single composite curve irrespective of the values of M_w and T below Θ when $A_2^{(HW)}M_w^{1/2}$ is plotted against the recalculated z (for a given polymer). The deviation of the $A_2M_w^{1/2}$ vs z plot or the A_2 vs $|\tau|$ plot from the two-parameter theory prediction previously reported arises not only from the effect of chain ends but also from the previous assumption of the proportionality of β and hence z to τ. The present and literature findings of the M independence of A_2 itself for a-PS (except for small M) below Θ are due to an accidental cancellation of the M dependence of $A_2^{(HW)}$ (through the function h) by that of $A_2^{(E)}$. (Note that the M dependence of A_2 in the oligomer region below and above Θ arises from the fact that $A_2^{(HW)}$ does not depend on M but $A_2^{(E)}$ does there.) Thus it is important to note that whether A_2 does or does not depend on M (except for small M) below Θ may probably depend on a given polymer–solvent system.

In the present work, we have not considered explicitly the ternary-cluster terms in A_2 and α_S, following the previous discussion.[1] The present results indicate that the (effective) binary-cluster approximation is actually good enough as far as only A_2 and α_S are concerned. It should be mentioned that at least in the oligomer region such that there are no intramolecular excluded-volume effects, ternary-cluster interactions never occur in A_2 and α_S because of chain stiffness.

References and Notes

(1) Yamakawa, H. *Macromolecules* **1993**, *26*, 5061.
(2) Yamakawa, H. *Macromolecules* **1992**, *25*, 1912.
(3) Yamakawa, H. *Annu. Rev. Phys. Chem.* **1984**, *35*, 23.
(4) Yamakawa, H. In *Molecular Conformation and Dynamics of Macromolecules in Condensed Systems*; Nagasawa, M., Ed.; Elsevier: Amsterdam, 1988; p 21.
(5) Tong, Z.; Ohashi, S.; Einaga, Y.; Fujita, H. *Polym. J.* **1983**, *15*, 835. A similar result has been obtained for polyisoprene in dioxane by: Takano, N.; Einaga, Y.; Fujita, H. *Polym. J.* **1985**, *17*, 1123. See also: Fujita, H. *Macromolecules* **1988**, *21*, 179.
(6) Perzynski, R.; Delsanti, M.; Adam, M. *J. Phys.* **1987**, *48*, 115.
(7) Yamakawa, H. *Modern Theory of Polymer Solutions*; Harper & Row: New York, 1971.
(8) Yamakawa, H.; Abe, F.; Einaga, Y. *Macromolecules* **1993**, *26*, 1898.
(9) Einaga, Y.; Abe, F.; Yamakawa, H. *Macromolecules* **1993**, *26*, 6243.
(10) Abe, F.; Einaga, Y.; Yamakawa, H. *Macromolecules* **1994**, *27*, 3262.
(11) Miyaki, Y. Ph.D. Thesis, Osaka University, 1981.
(12) Konishi, T.; Yoshizaki, T.; Shimada, J.; Yamakawa, H. *Macromolecules* **1989**, *22*, 1921.
(13) Einaga, Y.; Koyama, H.; Konishi, T.; Yamakawa, H. *Macromolecules* **1989**, *22*, 3419.
(14) Abe, F.; Einaga, Y.; Yamakawa, H. *Macromolecules* **1993**, *26*, 1891.
(15) Horita, K.; Abe, F.; Einaga, Y.; Yamakawa, H. *Macromolecules* **1993**, *26*, 5067.
(16) Konishi, T.; Yoshizaki, T.; Saito, T.; Einaga, Y.; Yamakawa, H. *Macromolecules* **1990**, *23*, 290.
(17) Abe, F.; Einaga, Y.; Yoshizaki, T.; Yamakawa, H. *Macromolecules* **1993**, *26*, 1884.
(18) Koyama, H.; Yoshizaki, T.; Einaga, Y.; Hayashi, H.; Yamakawa, H. *Macromolecules* **1991**, *24*, 932.
(19) Yamada, T.; Yoshizaki, T.; Yamakawa, H. *Macromolecules* **1992**, *25*, 377.
(20) Rubingh, D. N.; Yu, H. *Macromolecules* **1976**, *9*, 681.
(21) Einaga, Y.; Abe, F.; Yamakawa, H. *J. Phys. Chem.* **1992**, *96*, 3948.

(22) Berry, G. C. *J. Chem. Phys.* **1966**, *44*, 4550.
(23) Bawn, C. E. H.; Freeman, R. F. J.; Kamalidin, A. R. *Trans. Faraday Soc.* **1950**, *46*, 862.
(24) Norisuye, T.; Fujita, H. *ChemTracts—Macromol. Chem.* **1991**, *2*, 293.
(25) Allen, G.; Gee, G.; Mangaraj, D.; Sims, D.; Wilson, G. J. *Polymer* **1960**, *1*, 467.
(26) Höcker, H.; Blake, G. J.; Flory, P. J. *Trans. Faraday Soc.* **1971**, *67*, 2251.
(27) Holder, G. A.; Whalley, E. *Trans. Faraday Soc.* **1962**, *58*, 2095.
(28) The result for $(\partial\tilde{n}/\partial c)_{T,p}$ of OS3 in cyclohexane at 34.5 °C reported in ref 9 is somewhat erroneous. The value obtained in the present work is 0.146 cm^3/g independently of c for $c <$ 0.15 g/cm^3. Thus the values of k_1 and k_2 for OS3 in Table 2 of ref 9, i.e., 0.153 and −0.052, should be replaced by 0.146 and 0, respectively. A reanalysis of the LS data in ref 9 yields 2.1×10^{-3} $cm^3\,mol/g^2$ and 372 for A_2 and M_w, respectively. The former is smaller than the value 3.3×10^{-3} $cm^3\,mol/g^2$ reported previously (Table 3 of ref 9) and the latter is close to the correct value 370.
(29) Domb, C.; Barrett, A. J. *Polymer* **1976**, *17*, 179.
(30) Miyaki, Y.; Fujita, H. *Macromolecules* **1981**, *14*, 742. See also ref 14.
(31) Yamakawa, H.; Fujii, M. *J. Chem. Phys.* **1973**, *58*, 1523.
(32) Park, I. H.; Wang, Q.-W.; Chu, B. *Macromolecules* **1987**, *20*, 1965.
(33) Park, I. H.; Fetters, L.; Chu, B. *Macromolecules* **1988**, *21*, 1178.